# Machine learning based fitting of Zernike polynomials for ASSI

Markus Schake, Gerd Ehret

*Physikalisch-Technische Bundesanstalt, Bundesallee 100, 38116 Braunschweig, Germany*

*mailto:markus.schake@ptb.de*

This contribution provides an introduction to the application of least square optimization algorithms in annular subaperture stitching interferometry. It contains a fast and straight forward formulation of the least squares optimization problem of global stitching and a simulation example of annular subaperture stitching.

## 1 Introduction

Accurate and robust measurement of aspherical surfaces is an increasingly common task in the optics industry. A lot of research has fostered advances in aspherical metrology by means of tactile and optical approaches [1]. A commonly applied method for optical measurement of aspherical surfaces is annular subaperture stitching interferometry (ASSI) [2, 3, 4]. This contribution presents the application of a machine learning based Zernike polynomial fitting algorithm [5] to the problem of annular subaperture stitching, which results in a straight forward formulation of the optimization problem. The wavefront aberrations occurring due to position misalignments between the subaperture recordings are dependent on the employed reference wavefront. For a plane reference wave the positioning error related aberrations are constrained to piston, x-tilt and y-tilt. In case of a spherical reference wave also an aberration in the power term may occur.

## 2 Hands-on implementation of ASSI

This section introduces a global surface stitching approach and the formulation of the associated optimization problem. Assuming the measurement of a rotationally symmetric object of unit radius $-1 \leq r \leq 1$ and azimuthal angle $0 \leq \theta \leq 2\pi$ in global polar coordinates employing a plane reference wavefront. The employed detector does not cover the full object but scans it in terms of $K$ annular subapertures on the radial intervals $r_k = [r_{k0}, r_{k1}]$ with $k = 1, \cdots, K$. These intervals may be distributed arbitrary, they may overlap or having gaps in between, but each sample point of the $K$ measured local wavefront subapertures $w(r_k, \theta, k)$ must be assigned to a radial and azimuthal position. According to [2, 3, 4] the sampled subapertures may be represented in terms of annular Zernike polynomials defined on the local radial intervals $[r_{k0}, r_{k1}]$. The contributions [3, 4] employ a Zernike fitting to the differences of overlapping subapertures in their common region to correct the local translational errors before employing a global model fitting. Since, overlapping is not required in the scope of this contribution the approach employed in [2] is chosen for the formulation of the fitting problem. Thereby, the global wavefront $W(r, \theta)$, which is the measured representative of the surface form, may be expressed as Eq. (1) and (2).

$$W(r,\theta) = \sum_{k=1}^{K} \sum_{i=1}^{L} a_{ki} Z_{ki}(r_k, \theta, k) \tag{1}$$

$$W(r,\theta) = \sum_{k=1}^{K} \sum_{i=1}^{M} b_{ki} Z_{ki}(r_k, \theta, k) + \sum_{i=M+1}^{L} B_i Z_i(r,\theta) \tag{2}$$

The local subaperture wavefronts, including positioning induced aberrations represented through $L$ Zernike annular polynomial coefficients $w(r_k, \theta, k) = \sum_{i=1}^{L} a_{ki} Z_{ki}(r_k, \theta, k)$, are retrieved from the experimentally recorded data by the least square fitting presented in [5]. They represent the training set or input point cloud of subaperture measurements. The connections between machine learning techniques and the employed fitting are outlined in [5]. Assuming $N$ sample points per subaperture $\vec{Y}_k$, the global wavefront may be expressed by a row vector of the sampled values $W(r,\theta) = [\mathbf{Y}] = \left[\vec{Y}_1, \cdots, \vec{Y}_K\right]^T$ with $[\mathbf{Y}]_{KN\times 1}$. It is not required to fit the sampled subaperture data into annular Zernike polynomials before employing it as input data. However, doing so allows to choose an arbitrary set of supporting values by evaluating the annular polynomials for a customized set of supporting points $(r_k, \theta)$ on the $k$-th subaperture and therefore choosing an arbitrary number of samples $N$ for the optimization. The idea of Eq. (2) is, that the global wavefront may also be described as the sum of the local misalignment aberrations of low order and a set of $L - M$ global Zernike coefficients $B_i$ describing the actual form of the measuring object relative to the reference wavefront. The sum of the local low order Zernike polynomials $\sum_{i=1}^{M} b_{ki} Z_{ki}(r_k, \theta, k)$ with $M$ coefficients in equation (2) accounts for the unknown positioning error induced wavefront aberrations in the $k$-th subaperture. Since in this contribution a plane reference wavefront is employed these aberrations are limited to piston and tilt and described by $M = 3$ Zernike coefficients. The global Zernike coefficients $B_i$ shall be retrieved employing all sample points from all subapertures. Thus, the Zernike polynomial $Z_i(r,\theta)$ is evaluated at each supporting point for which a value is assigned in the vector $[\mathbf{Y}]_{KN\times 1}$ and may be formulated in terms of the subaperture coordinates as $Z_i(r,\theta) = \sum_{k=1}^{K} Z_{ki}(r_k,\theta,k)$, considering $Z_{ki}(r_k,\theta,k) = 0\ \forall r \notin r_k$. Using this formulation Eq. (2) is expressed as follows.

$$\underbrace{W(r,\theta)}_{\mathbf{Y}} = \underbrace{\sum_{k=1}^{K}\left[\sum_{i=1}^{M} b_{ki} Z_{ki}(r_k,\theta,k) + \sum_{i=M+1}^{L} B_i Z_{ki}(r_k,\theta,k)\right]}_{\mathbf{X}\cdot\mathbf{P}} \tag{3}$$

The sum on the right side of Eq. (3) is written in a matrix notation as the product of the Zernike polynomial matrix $[\mathbf{X}]_{KN\times(KM+(L-M))}$ multiplied with the matrix of the unknown local and global Zernike coefficients $[\mathbf{P}]_{(KM+(L-M))\times 1}$. This yields the matrix representation of the linear optimization problem:

$$\underbrace{\begin{bmatrix} \vec{Y}_1 \\ \vdots \\ \vec{Y}_k \\ \vdots \\ \vec{Y}_K \end{bmatrix}}_{\mathbf{Y}} = \underbrace{\begin{bmatrix} \mathbf{Z}_{b1} & 0 & \cdots & 0 & \mathbf{Z}_{B1} \\ 0 & \ddots & & \vdots & \vdots \\ \vdots & & \ddots & 0 & \vdots \\ 0 & 0 & 0 & \mathbf{Z}_{bK} & \mathbf{Z}_{BK} \end{bmatrix}}_{\mathbf{X}} \underbrace{\begin{bmatrix} \vec{b}_1 \\ \vdots \\ \vec{b}_K \\ \vec{B} \end{bmatrix}}_{\mathbf{P}} \tag{4}$$

In Eq. (4) $[\mathbf{Z}_{bk}]_{N\times M}$ and $[\mathbf{Z}_{Bk}]_{N\times(L-M)}$ are the Zernike polynomials of the local and global coefficients evaluated for $(r_k,\theta)$ of the respective $k$-th subaperture. The coefficients vectors $\vec{b}_k$ and $\vec{B}$ are of dimension $M\times 1$ and $(L-M\times 1)$ respectively. Employing the approach presented in [5], the Zernike polynomial coefficients of the global wavefront $\vec{B}$ result immediately from Eq. (5).

$$\mathbf{P} = \left(\mathbf{X}^T\mathbf{X}\right)^{-1}\cdot\mathbf{X}^T\mathbf{Y} \tag{5}$$

## 3 Simulation and Conclusion

The global model fitting approach is applied to simulated subaperture measurements to yield the global topography results as shown in the figure. The simulated aspherical object is characterized by the radius $R_{as} = 94.6\,\mathrm{mm}$, the conic constant $\kappa = -23.2046$ and $A_4 = -6.86465\cdot 10^{-6}\,\mathrm{mm}^{-3}$, $A6 = -1.21832\cdot 10^{-8}\,\mathrm{mm}^{-5}$, $A8 = 2.22491\cdot 10^{-11}\,\mathrm{mm}^{-7}$, $A10 = -8.06098\cdot 10^{-14}\,\mathrm{mm}^{-9}$ [6]. The form of this aspherical surface is well described by a Zernike polynomial and therefore a suitable candidate for the fitting algorithm. The considered region has a diameter of $D = 35\,\mathrm{mm}$, which is mapped to the unit circle. Each of the $K = 8$ subapertures contains $N = 32000$ sample points distributed on an $80\times 400$ raster. The local and global Zernike polynomials are described by $M = 3$ and $L = 36$ coefficients. The difference between the retrieved global topography and the input design function yields a peak to valley residual of PV $\approx 114\,\mathrm{nm}$. This PV value mainly depends on the simulated translational errors between the subapertures, and the chosen number of Zernike coefficients when fitting the sampled subapertures. Employing no translational errors and choosing the number of coefficients properly for the surface form reduces the PV value significantly.

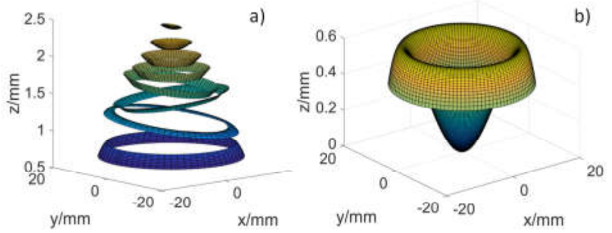


***Fig. 1** a) Virtually sampled subapertures of an aspherical object with various tilt and offset aberrations. b) Topography result employing the global model fitting approach with the sampled data from a) in* $[\mathbf{Y}]$.

Thus the global model fitting approach for ASSI presented in this contribution yields good results. However, due to the employed Zernike polynomial fitting it is generally difficult to handle rough surfaces of high spatial frequencies since the number of coefficients may not be increased limitless. Choosing high numbers of coefficients may cause singularities in the $\mathbf{X}$ matrix and affects the stability of the optimization. Also, as outlined in [1] the system is blind with respect to topography form changes in the regime of the low order Zernike coefficients describing the aberrations. This is obvious considering the lack of the lower order coefficients in the vector of global fitting parameters $\vec{B}$.

### References

[1] M. F. Küchel, "Interferometric measurement of rotationally symmetric aspheric surfaces," in *Optical Measurement Systems for Industrial Inspection VI*, P. H. Lehmann, ed., vol. 7389, pp. 389 – 422, International Society for Optics and Photonics (SPIE, 2009). URL https://doi.org/10.1117/12.830655.

[2] X. Hou, F. Wu, L. Yang, S. Wu, and Q. Chen, "Full-aperture wavefront reconstruction from annular subaperture interferometric data by use of Zernike annular polynomials and a matrix method for testing large aspheric surfaces," Appl. Opt. **45**(15), 3442–3455 (2006). URL https://doi.org/10.1364/AO.45.003442.

[3] X. Wang, L. Wang, L. Yin, B. Zhang, D. Fan, and X. Zhang, "Measurement of large aspheric surfaces by annular subaperture stitching interferometry," Chin. Opt. Lett. **5**(11), 645–647 (2007). URL http://col.osa.org/abstract.cfm?URI=col-5-11-645.

[4] Y. Wen, H. Cheng, H.-Y. Tam, and D. Zhou, "Modified stitching algorithm for annular subaperture stitching interferometry for aspheric surfaces," Appl. Opt. **52**(23), 5686–5694 (2013). URL https://doi.org/10.1364/AO.52.005686.

[5] D. R. Ibañez, J. A. Gómez-Pedrero, J. Alonso, and J. A. Quiroga, "Robust fitting of Zernike polynomials to noisy point clouds defined over connected domains of arbitrary shape," Opt. Express **24**(6), 5918–5933 (2016). URL https://doi.org/10.1364/OE.24.005918.

[6] R. Schachtschneider, I. Fortmeier, M. Stavridis, J. Asfour, G. Berger, R. B. Bergmann, A. Beutler, T. Blümel, H. Klawitter, K. Kubo, J. Liebl, F. Löffler, R. Meeß, C. Pruss, D. Ramm, M. Sandner, G. Schneider, M. Wendel, I. Widdershoven, M. Schulz, and C. Elster, "Interlaboratory comparison measurements of aspheres," Measurement Science and Technology **29**(5), 055,010 (2018). URL https://iopscience.iop.org/article/10.1088/1361-6501/aaae96.